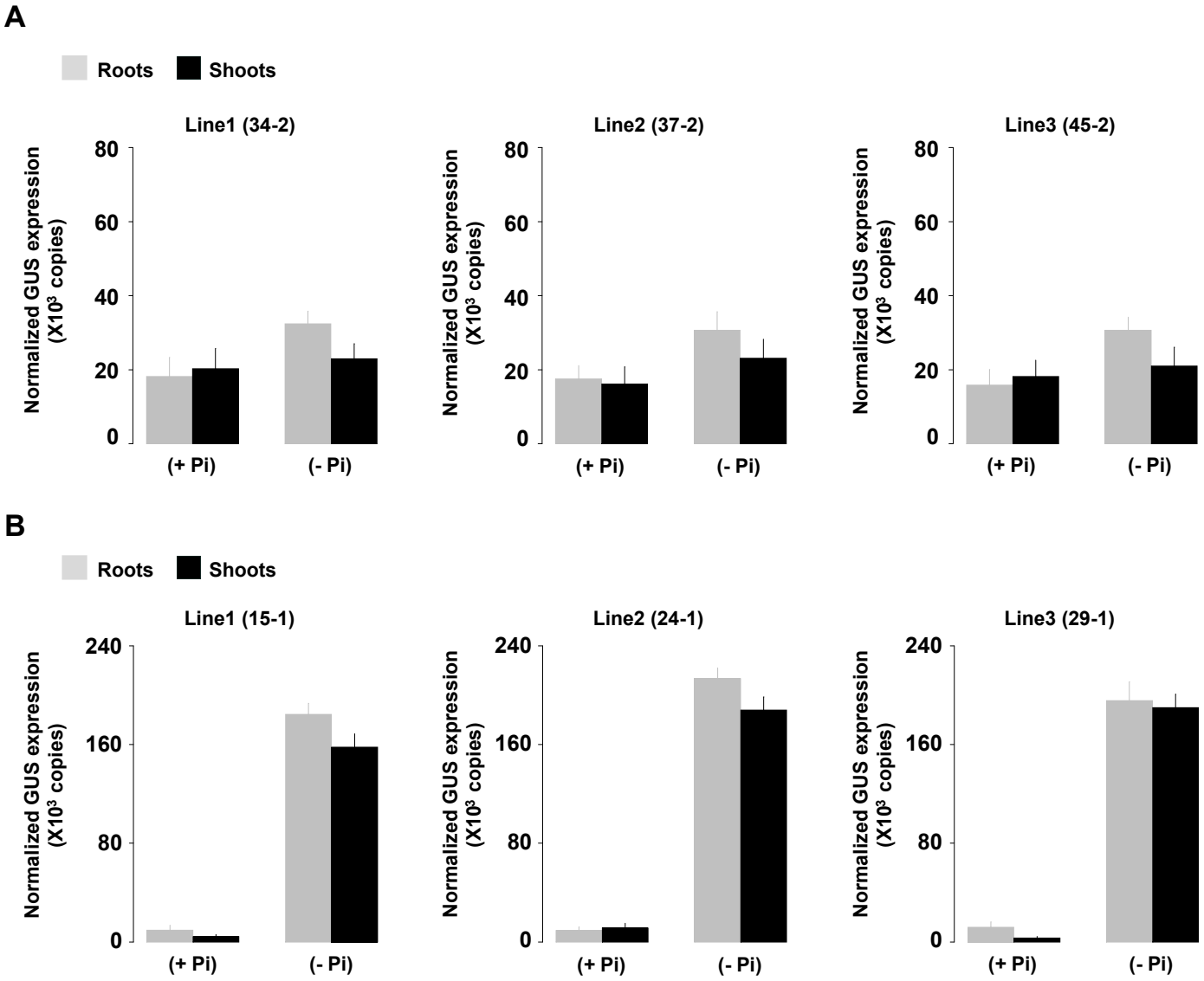

Supplemental Figure S1. Determination of the activity of the promoter of *PHO1;2* and *cis*-NAT$_{PHO1;2}$ in plants grown under Pi-sufficient and Pi-deficient conditions. Quantification of GUS expression level by (q)RT-PCR in Pro$_{OsPHO1;2\text{-S}}$:GUS **(A)** and Pro$_{cis\text{-NAT}}$:GUS **(B)** transgenic lines under Pi-sufficient (+Pi) or Pi-deficient (-Pi) condition. GUS expression was measured using mRNA extracted from roots or shoots. Three independent lines transformed with each construct were employed for GUS quantification. Data are means ± SE (n =3)

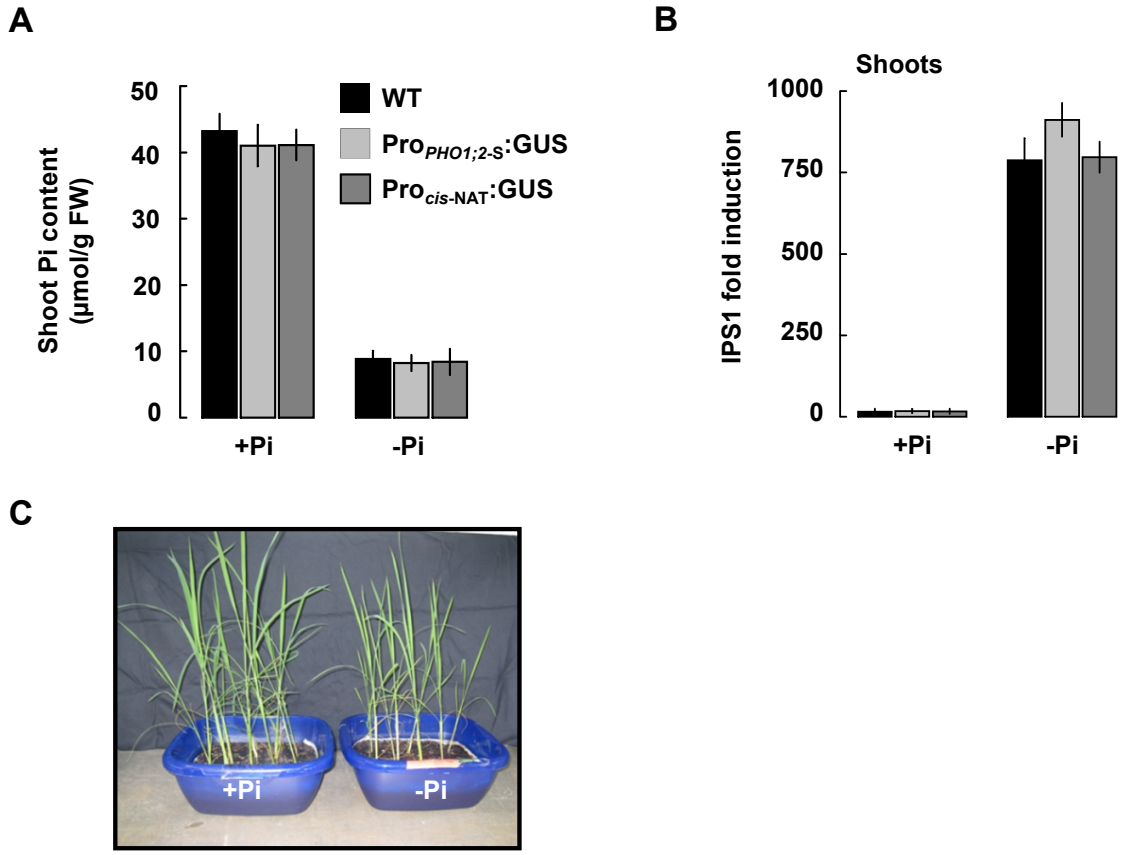

Supplemental Figure S2. Assessment of the Pi-deficiency status in the transgenic GUS lines. **(A)** Shoot Pi content of WT and transgenic GUS lines grown for 30 d in Pi-deficient medium. **(B)** Analysis of the Pi starvation-induced marker gene *IPS1* expression level in the shoots using (q)RT-PCR. Values are expressed as fold induction compared to the expression level from the first day of Pi-stress (day=0). **(C)** Morphological appearance of 30-d-old WT plants and transgenic GUS lines, grown hydroponically in Pi-deficient (-Pi) or Pi-sufficient (+Pi) medium. Data are means ± SE (n=4).

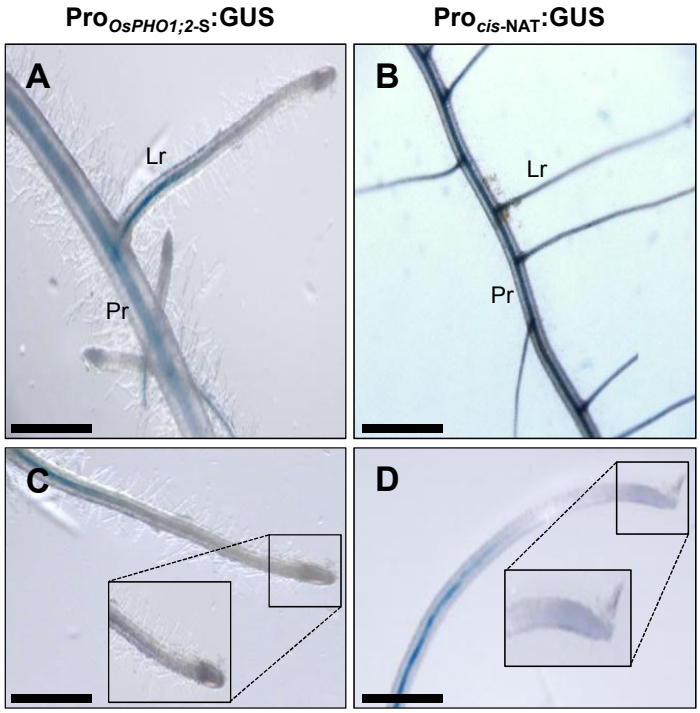

Supplemental Figure S3. GUS expression pattern in the roots of Pro$_{OsPHO1;2\text{-}S}$:GUS and Pro$_{cis\text{-}NAT}$:GUS transgenic lines. **(A)** Expression of *PHO1;2* in the primary (Pr) and lateral root (Lr) of Pro$_{OsPHO1;2\text{-}S}$:GUS lines grown in Pi-deficient medium. **(B)** Identical pattern in Pro$_{cis\text{-}NAT}$:GUS transgenic lines grown in Pi-deficient medium. **(C)** Root tip of the primary root shown in (A) containing the meristematic zone, showing no GUS staining. **(D)** Root tip of the primary root shown in (B) showing absence of GUS staining in the meristematic zone. Insets in (C) and (D) show magnified area. Pr, primary root; Lr, Lateral root. Scale bars: (A), (C) and (D): 0.3 cm; (B): 0.5 cm

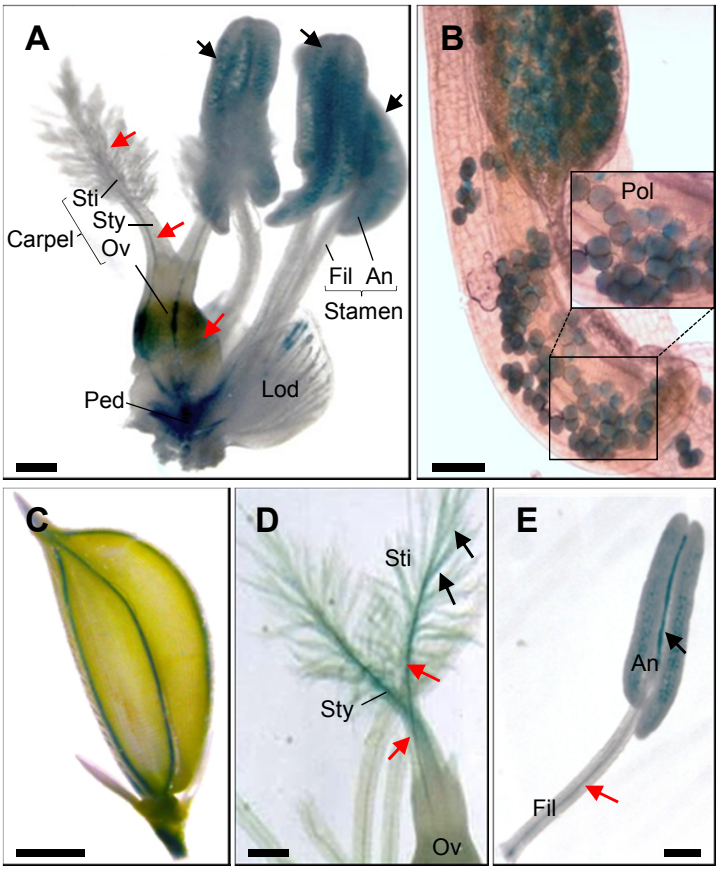

Supplemental Figure S4. Histochemical localization of GUS activity in the flower organs of rice plants transformed with the *cis*-NAT$_{PHO1;2}$ promoter:GUS vector. **(A)** Inner organs of mature transgenic rice flower revealed after removing the lemma and palea. Strong GUS signals were seen in anthers (black arrows) and in carpel (red arrows). **(B)** Anther showing high GUS expression in the mature pollen. Inset shows mature pollen. **(C)** GUS signal in spikelet hull. **(D)** GUS signal in stigma (black arrows) and style (red arrows). **(E)** GUS staining of transgenic anther showing expression in the vascular parenchyma where the base of the anther is connected to the filament (black arrow) and in the vascular bundle of the filament (red arrow). Scale bars: 0.25 mm (A), 100 µm (B), 1 mm (C), 0.5 mm (D), 200 µm (E). An, anther; Fil, Filament; Sti, Stigma; Sty, Style; Ov, Ovary; Lod, Lodicule; Ped, pedicel; Pol, Pollen.

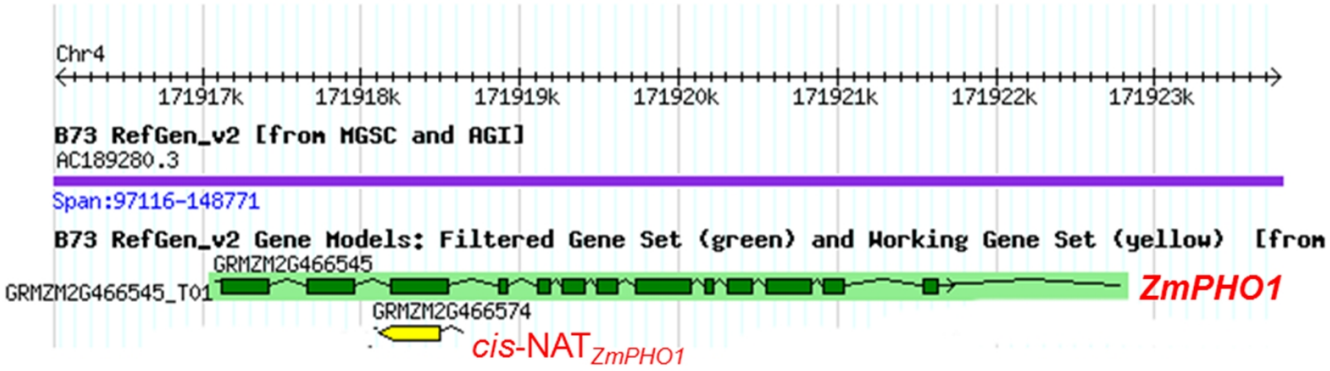

Supplemental Figure S5. *Cis*-NAT associated with the maize *PHO1* transcript. The exon-intron structure of the maize *ZmPHO1* homologue on chromosome 4, as predicted from the gene model GRMZM2G466545 on the Maize Genetics and Genomics database (http://www.maizegdb.org/), is shown in green. *Cis*-NAT$_{ZmPHO1}$ is shown in yellow and is based on gene model GRMZM2G466574 and a full-length cDNA (GenBank accession number FL468049.1).

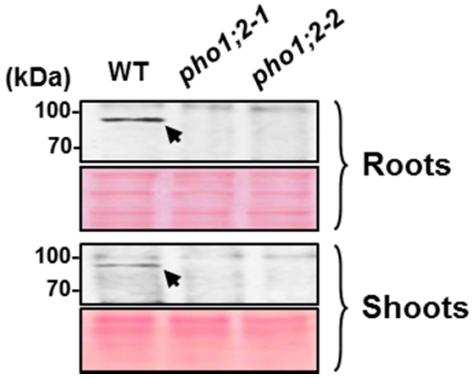

Supplemental Figure S6. Immunoblot analysis of PHO1;2 expression in wild type and *pho1;2* null mutants. Analysis performed on root and shoot microsomal extracts and a polyclonal antibody against PHO1;2. Ponceau S staining is shown in the bottom panel as a loading control. PHO1;2 was detected in one band as indicated by the black arrow.

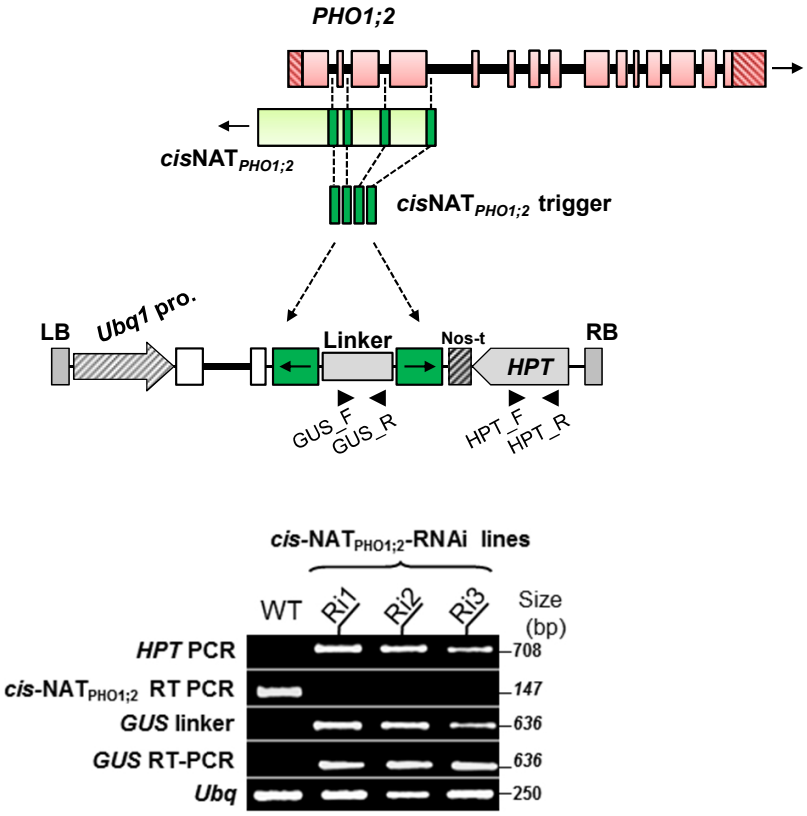

Supplemental Figure S7. Silencing of *cis*-NAT$_{PHO1;2}$. Schematic diagram of the RNAi cassette in the pANDA-RNAi*cis*NAT$_{PHO1;2}$ (upper panel) and molecular analysis of *cis*NAT$_{PHO1;2}$-RNAi plants by PCR and RT-PCR (lower panel). A chimeric 447 bp *cis*-NAT$_{PHO1;2}$ trigger was cloned in two orientations in pANDA vector to trigger RNAi. Transcripts of the RNAi-trigger region were designed to be expressed constitutively under the control of *pUbq* of the maize ubiquitin gene. Downstream of *pUbq*, the two unlabeled boxes represent exons and the thin line separating the exons marks an intron of the *Ubq* gene. Small arrowheads indicate position of primers used to detect the transgenes and test their effectiveness in silencing *cis*-NAT$_{PHO1;2}$. LB, left T-DNA border; NOS-t, nopalin synthase terminator; 35S, cauliflower mosaic virus promoter; HPT, hygromycin phosphotransferase; RB, right T-DNA border.

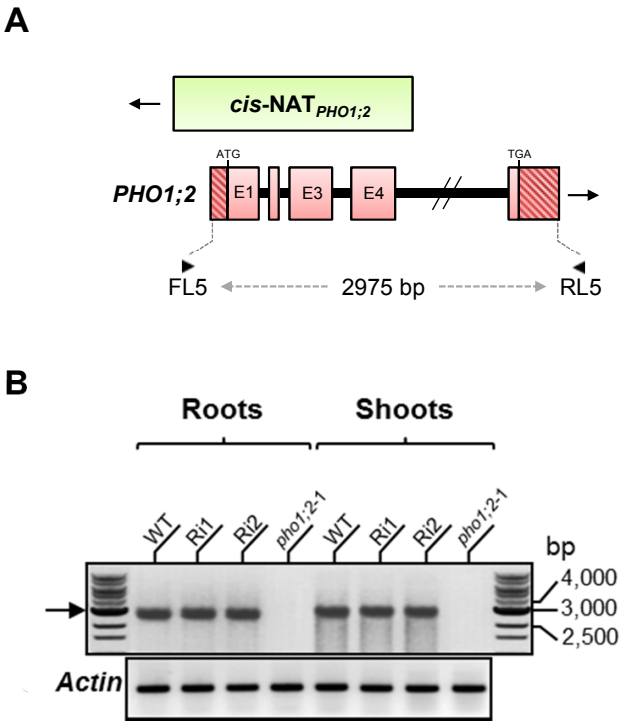

Supplemental Figure S8. RT-PCR analysis of *PHO1;2* transcripts. **(A)** Genomic organization of *PHO1;2* showing the position of the primers used for RT-PCR. Exons are indicated by open red boxes (with exons 1, 3 and 4 indicated as E1, E3 and E4, respectively), 3' and 5' UTRs by red hatched boxes, introns as black lines and location of the FL5 and RL5 primers by arrow heads. **(B)** RT-PCR analysis performed on RNAs extracted from roots and shoots of RNAi mutants, *pho1;2* mutant and WT plants. PCR primers FL5 and RL5 generate an amplification product of 2975 bp corresponding to *PHO1;2* full-length transcript, including 174 and 356 bp of the 5' and 3'UTR, respectively, based on the cDNA clone AK100323.

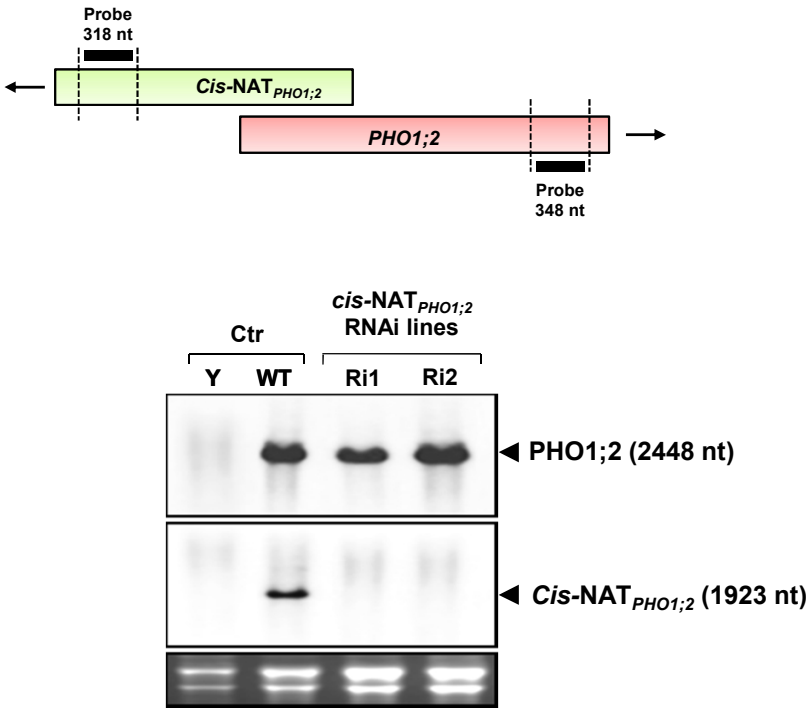

Supplemental Figure S9. RNA blot analysis of transgenic lines expressing an RNAi construct against the *cis*-NAT$_{PHO1.2}$. Eight micrograms of total RNA obtained from roots of wild-type (WT) and *cis*-NAT$_{PHO1;2}$ RNAi lines (Ri1 and Ri2) was subjected to analysis. A DIG-labeled antisense probe for either *PHO1;2* or *cis*-NAT$_{PHO1;2}$ was used as the hybridization probe (upper panel). The 18S and 28S ribosomal RNAs are shown after staining the agarose gel with ethidium bromide. Yeast RNA (Y) was used as negative control.

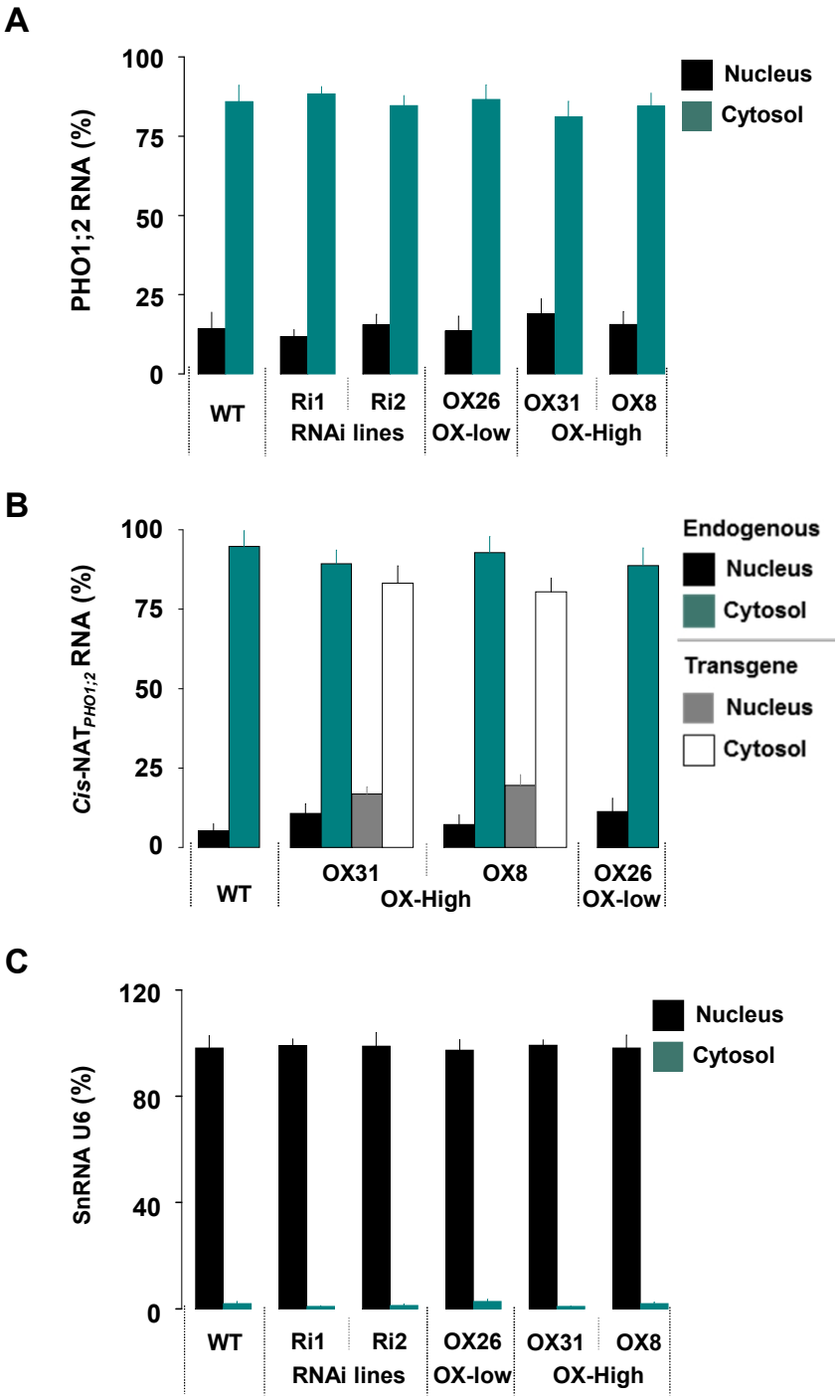

Supplemental Figure S10. Analysis of *PHO1.2* and $NAT_{PHO1.2}$ export from the nucleus. (q)RT-PCR analysis was performed using RNA extracted from the nucleus or cytosol of rice protoplasts. **(A)** Quantification of *PHO1;2* mRNA. **(B)** Quantification of *cis*-$NAT_{PHO1;2}$ (endogenous and transgenic modc*is*-$NAT_{PHO1;2}$). **(C)** Quantification of U6 small nuclear RNA (snRNA), used as a control for the efficiency of the nucleo-cytoplasmic fractionation. The mRNA percentage is defined as the amount of RNA quantified in the cytoplasmic or nucleic fraction divided by the total RNA quantified. Quantitation of three independent experiments is shown. Data are means ± SE (n =3).

Supplemental table 1: Primers used in this work

Purpose	Primer code	Amplicon size (pb)	Oligonucleotide Sequences (5′→3′)	
			Forward primer (F)	Reverse primer (R)
Promoter-GUS construction				
• $Pro_{OsPHO1;2\text{-}S}$:GUS	$P_{1;2S}$ F + R	1980	TGCGCCACTATCCGACCAAC	TTCCTCGTTGCAGCAGCAGC
• $Pro_{Cis\text{-}NAT}$:GUS	$P_{1;2as}$ F + R	2000	CAGGCAAAGCATTGGCATAG	ATTGTCTTCTATGCCATGCA
Strand specific absolute (q)RT-PCR				
• PHO1;2	F4 + R4	193	CGCCTAGCATGGACTGAGAGTGT	GTTCACGGAATGGTAATGGGACA
• Cis-$NAT_{PHO1;2}$ (Endogenous)	F3 + T3	147	GGCTACTAGCTTGGTGCTCTTCTCC	GCTAGCTAGCTCTACCTAATATTG
• Cis-$NAT_{PHO1;2}$ (Transgenic)	F3 + E3	208	GGCTACTAGCTTGGTGCTCTTCTCC	CTCGGAGATGAGCTTCTGCT
• IPS1(Induced-P-starvation gene1)	IPS1_F + R	60	TCCAAATAAAAGCACCCAATG	GAGCATACGTGGGCTTAAGAG
• GUS (β-glucuronidase gene)	GUS_F + R	211	CAACGGGGAAACTCAGCAAG	AGCGTCGCAGAACATTACAT
Detection of transcripts by RT-PCR				
• Full length PHO1;2	FL5 + RL5	2975	CGAGATCATCCCTGCCTGCC	GTGCATATGAATTCATGGAA
• Cis-$NAT_{PHO1;2}$	AS1 + AS2	338	TCTTCTTCTTCCTCGTTGCAG	CAAATTTCGCTGCATGCTTA
• Actin (Rice actin gene)	Actin_F + R	465	ATGCTCTCCCCCATGCTATC	TCTTCCTTGCTCATCCTGTC
Northern-Blot				
• PHO1;2 Probe	B12+B13	348	CTGCAACACCAACACCATTC	ACATTTGAACAACGTTGGCA
• Cis-$NAT_{PHO1;2}$ Probe	B14+B15	313	ATGGTCGATCCCCACTATGT	CAACCGTCCTGCCTTGTTAG
Confirmation of the RNAi construct				
• HPT (Hygromycin resistance gene)	HPT_F + R	708	CGAAGAATCTCGTGCTTTCAGC	AGCATATACGCCCGGAGTCG
• GUS linker / GUS RT-PCR	GUS_F + R	636	CATGAAGATGCGGACTTACG	ATCCACGCCGTATTCGG
• Ubq (Rice Ubiquitin gene)	Ubq_F + R	250	CCAGGACAAGATGATCTGCC	AAGAAGCTGAAGCATCCAGC
Detection of RNA editing variants	P_edit_F + R	1205	CTTTCCTGCATCCATCCATC	TTCTTCAATATTTTGGTGAAAGC
Detection of alternatively spliced transcripts by RT-PCR	Prim_A + B	243	CTACAAGCGGCTCAAGAAGC	ACGAGCTCCCCTCTGTCC
	Prim_A + D	391	CTACAAGCGGCTCAAGAAGC	TTCACCTTCTCCAGCTCCTC
	Prim_A + F	791	CTACAAGCGGCTCAAGAAGC	GGTCTTGCCGTCCTTCTTC
	Prim_C + D	84	GGACAGAGGGGAGCTCGT	TTCACCTTCTCCAGCTCCTC
	Prim_C + F	484	GGACAGAGGGGAGCTCGT	GGTCTTGCCGTCCTTCTTC
	Prim_E + F	169	CTACCTCCTCTCCGGCCTCT	GGTCTTGCCGTCCTTCTTC
Nuclear fractionation				
U6 (Rice Small nuclear RNA U6)	U6_F + R	175	GGAAGGACCTGAGCGTATGA	TTGTACGTGTCATCCTTGCG